

## **Dynamic Characteristics of Multi-functional Composite Shells Subjected to Electromagnetic and Thermal Fields**

\*Ohseop Song<sup>1)</sup>, Sang-Yun Park<sup>2)</sup>, Sung-Kyun Kim<sup>3)</sup>, and Jong Woon Choi<sup>4)</sup>

<sup>1), 2)</sup> *Dept. of Mechanical Engr., Chungnam National Univ., Daejeon, 305-764, Korea*

<sup>3)</sup> *Korea Atomic Energy Research Institute, Daejeon, 305-353, Korea*

<sup>4)</sup> *Korea Intellectual Property Office, Daejeon, 302-701, Korea*

*1) [songos@cnu.ac.kr](mailto:songos@cnu.ac.kr)*

### **ABSTRACT**

The free vibration analysis of cross-ply laminated composite shells subjected to a combination of magnetic and thermal fields is performed in the framework of the first-order shear deformable theory (FSDT). Coupled equations of motion for the analysis are obtained from electro-magnetic equations (Faraday's law, Ampere's law, Ohm's law, and Lorentz equations) and thermal equations which are involved in constitutive equations. The variations in the free vibration characteristics of composite shells with the applied magnetic field, temperature gradient, and geometric parameters are investigated, and pertinent conclusions are drawn.

### **1. Introduction**

Electromagnetic materials and structures are widely studied and applied in the fields of the aerospace industry, nuclear power plants, magnetic suspension systems, and electromechanical devices such as micro-actuators. Therefore, the dynamic behavior of a system subjected to a combined electromagnetic-thermal field constitutes one of the most interesting fields of study for researchers [1, 2].

This coupling between electromagnetic-thermal-elasticity for different stacking sequences of laminated composite structures should be considered in the design of such structures and systems.

Qin [3, 4] carried out pioneering research work on the nonlinear responses and stability of isotropic/composite cylindrical shells. Tsai and Wu [5] performed a free vibration analysis of a functionally graded magnetic-electric-elastic shell with an open-circuit

---

1) Professor  
2) Graduate Student  
3) Senior Researcher  
4) Patent Examiner

surface condition.

Yoon [6] performed the topology optimization that considered the electro-fluid-thermal-compliant couplings for a micro-actuator.

In this study, a free vibration analysis of a cross-ply laminated composite cylindrical shell is performed when it is subjected to a combined electromagnetic and thermal field.

## 2. Equations of Motion

### 2.1 Displacement field

Figure 1 shows the geometry and curvilinear coordinate system  $(x, \theta, z)$  of a cross-ply laminated composite cylindrical shell. The shell is subjected to both a magnetic field in the axial direction and temperature variation beyond its stress-free state.

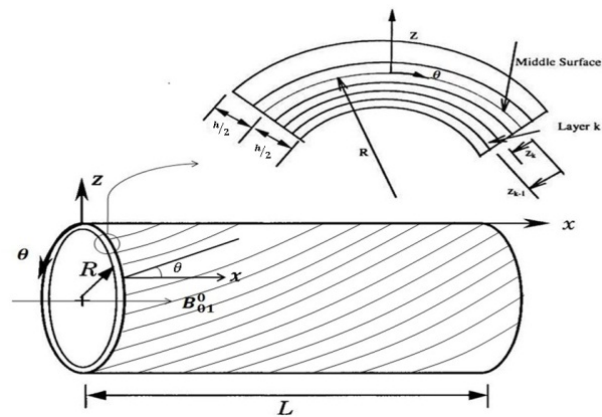


**Fig. 1 Geometry of laminated composite shells**

The following geometric and kinematic assumptions are incorporated in the modeling of a laminated composite cylindrical shell:

- (a) Layers are perfectly bonded to each other, and their thicknesses are identical.
- (b) Both the thickness-to-radius ratio and the thickness-to-length ratio are very small.
- (c) The transverse shear effect is included.

The displacement field of a thin shell in the framework of the FSDT is given by [7]

$$U_1(x, \theta, z, t) = u_1(x, \theta, t) + z\beta_1(x, \theta, t) \quad (1a)$$

$$U_2(x, \theta, z, t) = u_2(x, \theta, t) + z\beta_2(x, \theta, t) \quad (1b)$$

$$U_3(x, \theta, z, t) = u_3(x, \theta, t) \quad (1c)$$

where  $u_1, u_2, u_3$  are 2D kinematic variables in  $x, \theta, z$  directions, respectively.  $\beta_1$  and  $\beta_2$  represent the rotation about  $\theta$  and  $x$  axis, respectively.

## 2.2 Electromagnetic field equations

The electromagnetic equations are derived from the generalized Maxwell equations as [2]:

$$\text{Faraday's law} \quad \nabla \times \mathbf{E} = -\dot{\mathbf{B}} \quad (2a)$$

$$\text{Ampere's law} \quad \nabla \times \mathbf{H} = \mathbf{J} \quad (2b)$$

$$\text{Ohm's law} \quad \mathbf{J} = \mathbf{G}(\mathbf{E} + \dot{\mathbf{V}} \times \mathbf{B}) \quad (2c)$$

$$\text{Lorentz force} \quad \mathbf{f} = \mathbf{J} \times \mathbf{B} \quad (2d)$$

$$\text{Magnetic field intensity} \quad \mathbf{B} = \mu_0 \mathbf{H} \quad (2e)$$

where  $\mathbf{E}$  denotes the electric field vector,  $\mathbf{H}$  is the magnetic field vector,  $\mathbf{J}$  is the current density vector, and  $\mathbf{B}$  is the magnetic induction intensity vector.  $\mathbf{f}$  is the Lorentz force vector per unit volume,  $\mu_0$  is the permeability in vacuum. Matrix  $\mathbf{G}$  represents the electric conductivity matrix of a composite shell.

$$\mathbf{G} \equiv \begin{bmatrix} g_{11} & g_{12} & 0 \\ g_{12} & g_{22} & 0 \\ 0 & 0 & g_{33} \end{bmatrix} \quad (3)$$

where  $g_{11} = g_1 \cos^2 \theta + g_2 \sin^2 \theta$ ,  $g_{33} = g_3$ ,  $g_{22} = g_2 \cos^2 \theta + g_1 \sin^2 \theta$ ,  $g_{12} = (g_1 - g_2) \sin \theta \cos \theta$ ,  $g_i (i = 1, 2, 3)$  is the electric conductivity coefficient in the principle direction of the fiber.

## 2.3 Equations of Motion and Boundary Conditions

The equations of motion and the boundary conditions for a simply supported cross-ply laminated composite cylindrical shell are derived via Hamilton's variation principle [8].

The magnetic field is applied in the axial direction, and the temperature gradient exists beyond the stress-free state.

Hamilton's principle:

$$\delta J = \delta \int_{t_0}^{t_1} [T - U + W_e] dt = 0 \quad (4)$$

$$\text{at } t = t_0, t = t_1: \delta u_i = 0, \delta \beta_\zeta = 0 (i = 1, 2, 3 \zeta = 1, 2)$$

(1) Equations of motion:

$$\begin{aligned} \delta u_1: A_{11} u_{1,11} + A_{12} \left( \frac{1}{R} u_{2,12} + \frac{1}{R} u_{3,1} \right) + A_{66} \left( \frac{1}{R} u_{2,12} + \frac{1}{R^2} u_{1,22} \right) \\ - m_1 \ddot{u}_1 + \int_{\alpha_3} f_1 d\alpha_3 = 0 \end{aligned} \quad (5a)$$

$$\begin{aligned} \delta u_2: & A_{66} \left( u_{2,11} + \frac{1}{R} u_{1,12} \right) + A_{12} \frac{1}{R} u_{1,12} + A_{22} \left( \frac{1}{R^2} u_{2,22} + \frac{1}{R^2} u_{3,2} \right) \\ & - m_1 \ddot{u}_2 + \int_{\alpha_3} f_2 d\alpha_3 = 0 \end{aligned} \quad (5b)$$

$$\begin{aligned} \delta u_3: & A_{55} (\beta_{1,1} + u_{3,11}) + A_{44} \left( \frac{1}{R} \beta_{2,2} + \frac{1}{R^2} u_{3,22} \right) - \frac{1}{R} A_{12} u_{1,1} \\ & - A_{22} \left( \frac{1}{R^2} u_{2,2} + \frac{1}{R^2} u_3 \right) - A_{11}^\alpha \Theta u_{3,11} - \frac{2}{R} A_{12}^\alpha \Theta u_{3,12} - \frac{1}{R^2} A_{22}^\alpha \Theta u_{3,22} \\ & - m_1 \ddot{u}_3 + \int_{\alpha_3} f_3 d\alpha_3 = 0 \end{aligned} \quad (5c)$$

$$\begin{aligned} \delta \beta_1: & D_{11} \beta_{1,11} + D_{12} \frac{1}{R} \beta_{2,12} + D_{66} \left( \frac{1}{R^2} \beta_{1,22} + \frac{1}{R} \beta_{2,12} \right) - A_{55} (\beta_1 + u_{3,1}) \\ & - m_3 \ddot{\beta}_1 + \int_{\alpha_3} f_1 \alpha_3 d\alpha_3 = 0 \end{aligned} \quad (5d)$$

$$\begin{aligned} \delta \beta_2: & D_{66} \left( \beta_{2,11} + \frac{1}{R} \beta_{1,12} \right) + D_{12} \frac{1}{R} \beta_{1,12} + D_{22} \frac{1}{R^2} \beta_{2,22} - A_{44} \left( \beta_2 + \frac{1}{R} u_{3,2} \right) \\ & - m_3 \ddot{\beta}_2 + \int_{\alpha_3} f_2 \alpha_3 d\alpha_3 = 0 \end{aligned} \quad (5e)$$

where the Lorentz forces and momenta per unit area are as follows:

$$\int_{-h/2}^{h/2} f_1 \alpha_3 = 0 \quad (6a)$$

$$\int_{-h/2}^{h/2} f_2 d\alpha_3 = -h M_0 [g_{33}] \dot{u}_2 (B_{01}^0)^2 = -h \bar{g}_{33} \dot{u}_2 (B_{01}^0)^2 \quad (6b)$$

$$\int_{-h/2}^{h/2} f_3 d\alpha_3 = -h M_0 [g_{22}] \dot{u}_3 (B_{01}^0)^2 = -h \bar{g}_{22} \dot{u}_3 (B_{01}^0)^2 \quad (6c)$$

$$\int_{-h/2}^{h/2} \alpha_3 f_1 dx_3 = 0 \quad (6d)$$

$$\int_{-h/2}^{h/2} \alpha_3 f_2 d\alpha_3 = -h M_2 [g_{33}] \dot{\beta}_2 (B_{01}^0)^2 = -C_{22}^g \dot{\beta}_2 (B_{01}^0)^2 \quad (6e)$$

(2) Boundary conditions:

at  $x = 0, L$ :

$$\begin{aligned} \delta u_1: & A_{11} u_{1,1} + A_{12} \left( \frac{1}{R} u_{2,2} + \frac{1}{R} u_3 \right) = 0, \\ \delta u_2: & u_2 = 0, \\ \delta u_3: & u_3 = 0, \\ \delta \beta_1: & D_{11} \beta_{1,1} + D_{12} \frac{1}{R} \beta_{2,2} = 0, \end{aligned} \quad (7)$$

$$\delta\beta_2: \beta_2 = 0.$$

at  $\theta = 0, 2\pi$  :

$$\begin{aligned} \delta u_1: u_1 &= 0, \\ \delta u_2: A_{12} \frac{1}{R} u_{1,1} + A_{22} \left( \frac{1}{R^2} u_{2,2} + \frac{1}{R^2} u_3 \right) &= 0, \\ \delta u_3: u_3 &= 0, \\ \delta\beta_1: \beta_1 &= 0, \\ \delta\beta_2: D_{12} \frac{1}{R} \beta_{1,1} + D_{22} \frac{1}{R^2} \beta_{2,2} &= 0. \end{aligned} \quad (8)$$

### (3) Discretized equations of motion

The governing equations are discretized through the extended Galerkin method. The following trial functions are chosen to satisfy boundary conditions as much as possible.

$$u_1(x, \theta, t) = \sum_{n=1}^{\infty} \sum_{m=1}^{\infty} \cos \alpha_m x \sin \beta_n \theta \cdot q(t) \quad (9a)$$

$$u_2(x, \theta, t) = \sum_{n=1}^{\infty} \sum_{m=1}^{\infty} \sin \alpha_m x \cos \beta_n \theta \cdot q(t) \quad (9b)$$

$$u_3(x, \theta, t) = \sum_{n=1}^{\infty} \sum_{m=1}^{\infty} \sin \alpha_m x \sin \beta_n \theta \cdot q(t) \quad (9c)$$

$$\beta_1(x, \theta, t) = \sum_{n=1}^{\infty} \sum_{m=1}^{\infty} \cos \alpha_m x \sin \beta_n \theta \cdot q(t) \quad (9d)$$

$$\beta_2(x, \theta, t) = \sum_{n=1}^{\infty} \sum_{m=1}^{\infty} \sin \alpha_m x \cos \beta_n \theta \cdot q(t) \quad (9e)$$

where  $\alpha_m = \frac{m\pi}{L}$ ,  $\beta_n = n$ .

Substitution of Eqs. (9) into the equations of motion in conjunction with the boundary conditions yields the following discretized equations of motion:

$$[M]\ddot{\mathbf{q}}(t) + [C]\dot{\mathbf{q}}(t) + [K]\mathbf{q}(t) = 0 \quad (10)$$

The above equations of motion are transformed into a state equation as follows:

$$[M]^* \dot{\mathbf{x}}(t) + [K]^* \mathbf{x}(t) = 0 \quad (11)$$

where  $[M]^* = \begin{bmatrix} M & 0 \\ 0 & -K \end{bmatrix}$ ,  $[K]^* = \begin{bmatrix} C & K \\ K & 0 \end{bmatrix}$ ,  $\mathbf{x} = \begin{Bmatrix} \dot{\mathbf{q}} \\ \mathbf{q} \end{Bmatrix}$

The solution to Eq. (11) has the form  $\mathbf{x}(t) = e^{\lambda t} \mathbf{x}$ , and Eq. (11) is transformed into an eigenvalue problem as:

$$\lambda[\mathbf{M}]^* \mathbf{x} + [\mathbf{K}]^* \mathbf{x} = 0 \quad (12)$$

where  $\lambda$  denotes complex eigenvalues,  $\lambda_r = \sigma_r \pm i\omega_{dr}$ , where  $\sigma_r$  is the damping and  $\omega_{dr}$  is the damped natural frequency.  $\mathbf{x}$  is the eigenvector (mode shapes).

### 3. Numerical Results and Discussion

Table 1 shows a comparison of the natural frequencies in the present analysis with those in Reference [9] for a stacking sequence of  $[0^\circ \ 90^\circ \ 90^\circ \ 0^\circ]$  to validate the extended Galerkin method used in the present analysis.

Fig. 2 shows the variations in the fundamental frequency and the first damping ratio with magnetic field intensity  $B_{01}^0$ . As the magnetic field intensity  $B_{01}^0$  increases, the natural frequency decreases because the applied magnetic field increases the damping, as can be seen in Fig. (2b). The natural frequencies for the case of  $R = 10L$  are lower than for the case of  $R = 5L$ . In other words, the larger the radius of the shell is, the lower the natural frequencies are, assuming the length of the shell is fixed.

Fig. 3 shows the variation in the fundamental frequency with the temperature gradient for three different values of the magnetic field; the variation is observed to be almost linear. As the magnetic field or temperature gradient increases, the natural frequencies monotonically decrease because the temperature gradient affects the stiffness matrix  $[\mathbf{K}]$ , whereas the magnetic field produces a damping matrix  $[\mathbf{C}]$  (see Appendix A.2).

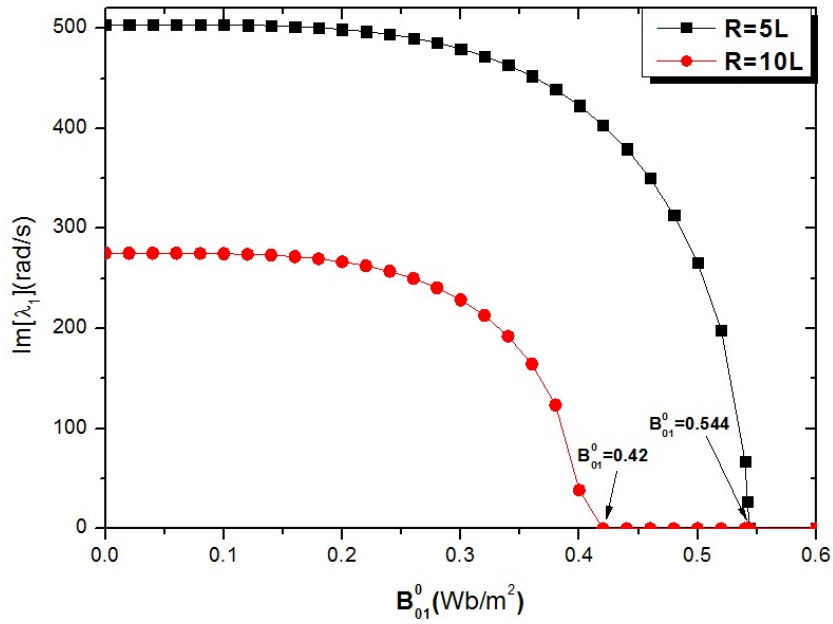
Fig. 4 is the same as Fig. 3; however, it shows the variation in the fundamental frequency with the magnetic field intensity for three different temperature gradients. Fig. 4 also indicates that the temperature gradient affects the values of the magnetic field intensity, which can make the natural frequencies to zero valued quantity.

Compared with a positive gradient, a negative temperature gradient requires a larger magnetic field to derive the natural frequency to zero.

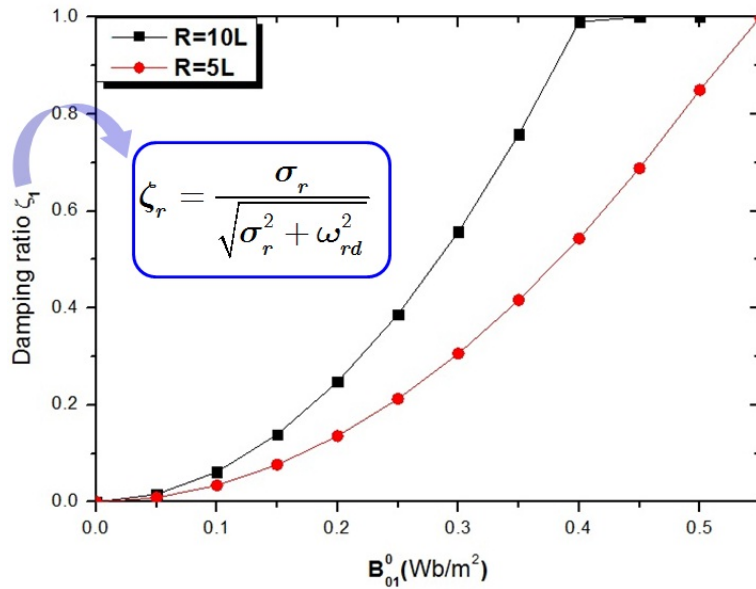
Fig. 5 reveals the effect of the stacking sequence on the variation in the fundamental natural frequency with the magnetic field. The stiffness quantities of the structure are greatly affected by the stacking sequences and the fiber angles.

**Table 1 Comparison of the natural frequencies with those in Reference [9] for a stacking sequence  $[0^\circ \ 90^\circ \ 90^\circ \ 0^\circ]$**

Present	Reference [9], Reddy	Error (%)
<b>Case 1 (<math>R = 5L</math>)</b>		0.39%
20.2803	20.361	
<b>Case 2 (<math>R = 10L</math>)</b>		0.4%
16.701	16.634	



(a)  $\text{Im} [\lambda_1]$



(b) 1<sup>st</sup> damping ratio  $\zeta_1$

**Fig. 2** Variation in the fundamental natural frequency and the first damping ratio with  $B_{01}^0$  ( $L = 100h, R = 10L, \frac{g_1}{g_2} = \frac{g_3}{g_0} = 3.0, \frac{g_2}{g_0} = 1.1$ )

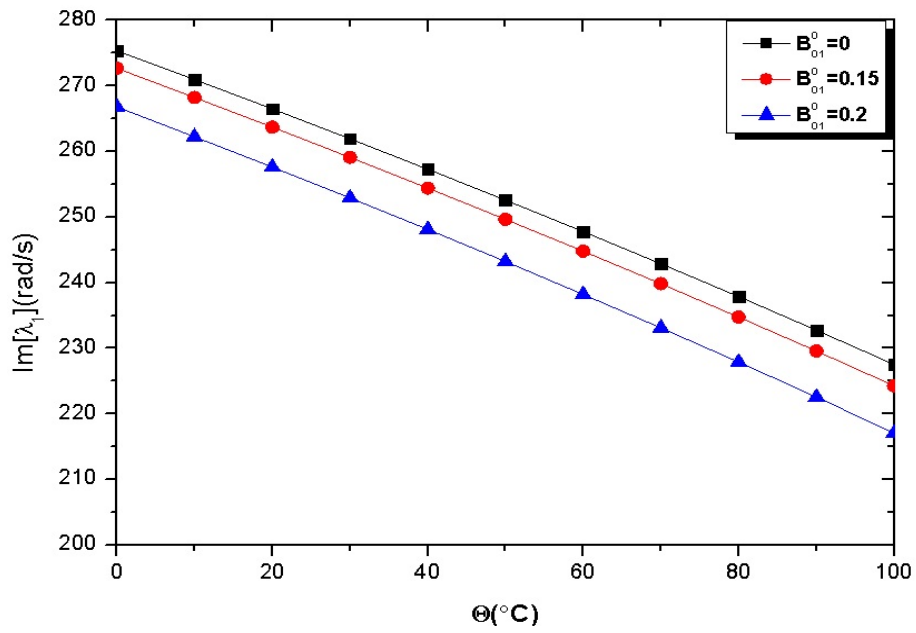


**Fig. 3** Variation in the fundamental natural frequency with  $\Theta$  for three different values of  $B_{01}^0$

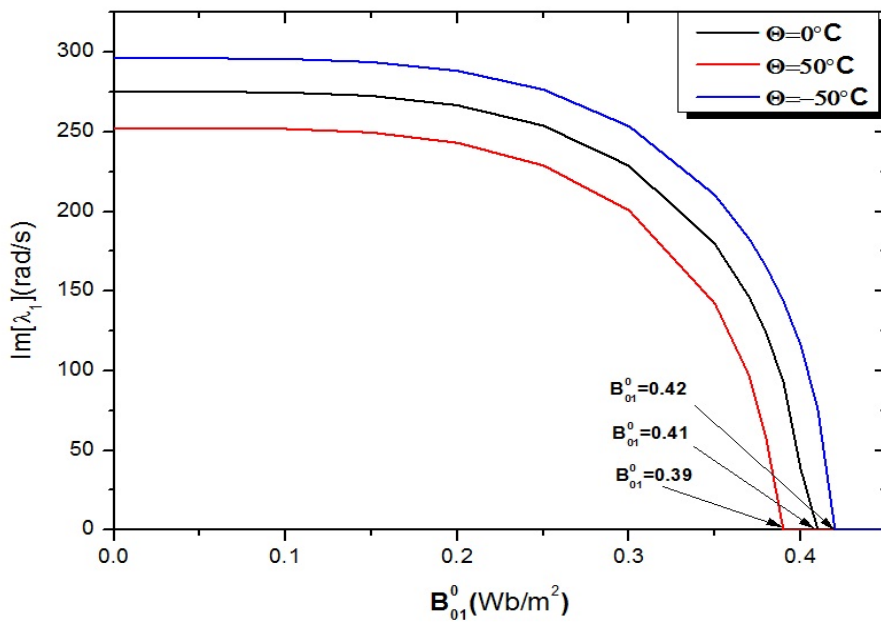


**Fig. 4** Variation in the fundamental natural frequency with  $B_{01}^0$  for three different values of  $\Theta$



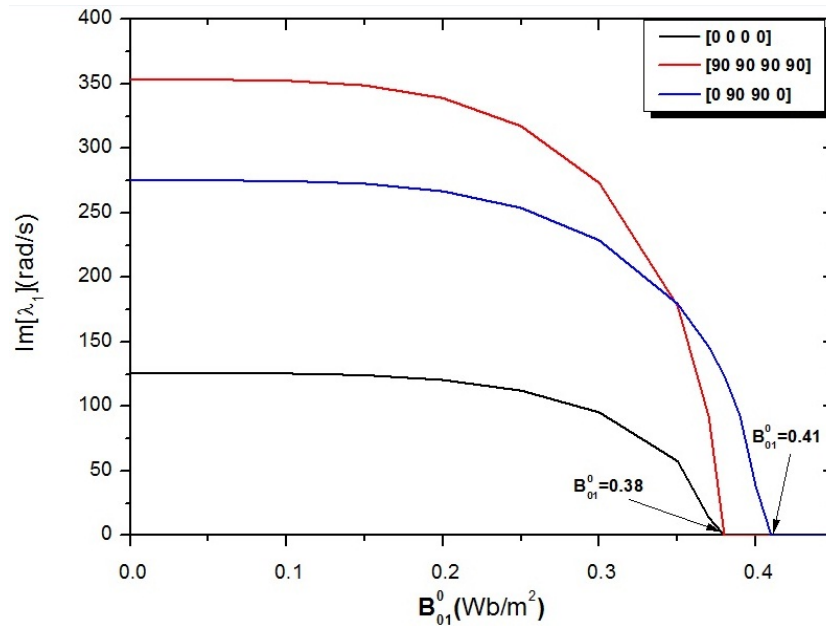


**Fig. 5 Variation in the fundamental natural frequency with  $B_{01}^0$  for three different stacking sequences**

#### 4. Conclusion

The dynamic characteristics of cross-ply laminated composite shells subjected to a combined magnetic and thermal field are performed. Coupled equations of motion for the analysis are obtained from electro-magnetic equations and thermal ones which are involved in the constitutive equations.

The variations in the free vibration characteristics of composite shells with the applied magnetic field, temperature gradient, radius ratio, and length of the shell are investigated, and pertinent conclusions are outlined.

#### References

- 1) Sung-Kyun Kim., Kune-Woo Lee., Jei-Kwon Moon., Jong-Woon Choi., Young-Jun Kim., Sang-Yun Park and Ohseop Song ,2011, Dynamic Characteristics of Composite Plate Subjected to Electromagnetic and Thermal Field, KSNVE, pp.536-546.
- (2) F.C. Moon, Magneto-Solid Mechanics, John Wiley and Sons, Ithaca, New York, 1984, pp. 288-296.
- (3) Zhanming Qin., Davresh Hasanyan, 2011, Fully non-linear magnetoelastic interactions of a circular cylindrical thin shell subject to electromagnetic fields, International Journal of Non-Linear Mechanics, pp. 425-435.

- (4) Zhanming Qin, 2010, Magneto-thermo-elasticity of an electroconductive circular cylindrical shell featuring nonlinear deformations, International Journal of Engineering Science, pp. 1797-1810.
- (5) Yi-Hwa Tsai and Chih-Ping Wu., 2008, Dynamic responses of functionally graded magneto-electro-elastic shells with open-circuit surface conditions, International Journal of Engineering Science, Vol.46, No.9, pp.843-857.
- (6) Yoon Gil Ho., 2010, Topology optimization considering the couplings of electro-fluid-thermal-compliant micro actuator, KSME, pp640-642 New York.
- (7) Werner Soedel., 2004, Vibrations of Shells and Plates 3rd Edition, Marcel Dekker Inc.
- (8) Reddy J.N., 2004, Mechanics of Laminated Composite Plates and Shells Theory and Analysis 2nd Edition, CRC Press, New York.
- (9) Reddy J.N., C.F.LIU, 1985 A higher-order shear deformation theory of laminated elastic shells, International Journal of Engineering Science, pp.319-330.

## Acknowledgement

This work is supported by the Basic Science Research Program through the National Research Foundation of Korea (NRF) funded by the Ministry of Education, Science and Technology (No.2011-0027000).

## Appendix

### A.1 Elements of matrices in Eqs. (10)

$$A_{ij} = \sum_{k=1}^{N_L} \bar{Q}_{ij}^{(k)} (z_{k+1} - z_k)$$

$$D_{ij} = \frac{1}{3} \sum_{k=1}^{N_L} \bar{Q}_{ij}^{(k)} (z_{k+1}^3 - z_k^3)$$

$$A_{11}^{\alpha} = \sum_{k=1}^{N_L} [A_{11}^{(k)} \alpha_{11}^{(k)} + A_{12}^{(k)} \alpha_{22}^{(k)} + A_{16}^{(k)} \alpha_{12}^{(k)}]$$

$$A_{12}^{\alpha} = \sum_{k=1}^{N_L} [A_{16}^{(k)} \alpha_{11}^{(k)} + A_{26}^{(k)} \alpha_{22}^{(k)} + A_{66}^{(k)} \alpha_{12}^{(k)}]$$

$$A_{22}^\alpha = \sum_{k=1}^{N_L} \left[ A_{12}^{(k)} \alpha_{11}^{(k)} + A_{22}^{(k)} \alpha_{22}^{(k)} + A_{26}^{(k)} \alpha_{12}^{(k)} \right]$$

$$m_1 = \sum_{k=1}^{N_L} \rho_0^{(k)} (z_{k+1} - z_k)$$

$$m_3 = \frac{1}{3} \sum_{k=1}^{N_L} \rho_0^{(k)} (z_{k+1}^3 - z_k^3)$$

## A.2 Mass [M], damping [C] and stiffness [K] matrices

$$M = \begin{bmatrix} M_{11} & 0 & 0 & 0 & 0 \\ 0 & M_{22} & 0 & 0 & 0 \\ 0 & 0 & M_{33} & 0 & 0 \\ 0 & 0 & 0 & M_{44} & 0 \\ 0 & 0 & 0 & 0 & M_{55} \end{bmatrix}, \quad C = \begin{bmatrix} 0 & 0 & 0 & 0 & 0 \\ 0 & C_{22} & 0 & 0 & 0 \\ 0 & 0 & C_{33} & 0 & 0 \\ 0 & 0 & 0 & 0 & 0 \\ 0 & 0 & 0 & 0 & C_{55} \end{bmatrix}, \quad K = \begin{bmatrix} K_{11} & K_{12} & K_{13} & 0 & 0 \\ K_{21} & K_{22} & K_{23} & 0 & 0 \\ K_{31} & K_{32} & K_{33} & K_{34} & K_{35} \\ 0 & 0 & K_{43} & K_{44} & K_{45} \\ 0 & 0 & K_{53} & K_{54} & K_{55} \end{bmatrix}$$

where

$$M_{11} = \int_{\Omega} m_1 \psi_1 \psi_1^T d\Omega, \quad M_{22} = \int_{\Omega} m_1 \psi_2 \psi_2^T d\Omega, \quad M_{33} = \int_{\Omega} m_1 \psi_3 \psi_3^T d\Omega,$$

$$M_{44} = \int_{\Omega} m_3 \psi_4 \psi_4^T d\Omega, \quad M_{55} = \int_{\Omega} m_3 \psi_5 \psi_5^T d\Omega.$$

$$C_{22} = (B_{01}^0)^2 \int_{\Omega} h \bar{g}_{33} \psi_2 \psi_2^T d\Omega, \quad C_{33} = (B_{01}^0)^2 \int_{\Omega} h \bar{g}_{22} \psi_3 \psi_3^T d\Omega$$

$$C_{55} = (B_{01}^0)^2 \int_{\Omega} C_{33}^g \psi_5 \psi_5^T d\Omega.$$

$$K_{11} = \int_{\Omega} \left( A_{11} \psi_{1,1} \psi_{1,1}^T - \frac{1}{R^2} A_{66} \psi_1 \psi_{1,22}^T \right) d\Omega$$

$$K_{12} = \int_{\Omega} \left( \frac{1}{R} A_{12} \psi_{1,1} \psi_{2,2}^T - \frac{1}{R} A_{66} \psi_1 \psi_{2,12}^T \right) d\Omega$$

$$K_{13} = \int_{\Omega} \left( \frac{1}{R} A_{12} \psi_{1,1} \psi_3^T \right) d\Omega, \quad K_{21} = \int_{\Omega} \left( \frac{1}{R} A_{12} \psi_{2,2} \psi_{1,1}^T - \frac{1}{R} A_{66} \psi_2 \psi_{1,12}^T \right) d\Omega$$

$$K_{22} = \int_{\Omega} \left( \frac{1}{R^2} A_{22} \psi_{2,2} \psi_{2,2}^T - A_{66} \psi_2 \psi_{2,11}^T \right) d\Omega, \quad K_{23} = \int_{\Omega} \left( \frac{1}{R^2} A_{22} \psi_{2,2} \psi_3^T \right) d\Omega$$

$$K_{31} = \int_{\Omega} \left( \frac{1}{R} A_{12} \psi_3 \psi_{1,1}^T \right) d\Omega, \quad K_{32} = \int_{\Omega} \left( \frac{1}{R^2} A_{22} \psi_3 \psi_{2,2}^T \right) d\Omega$$

$$\begin{aligned}
K_{33} &= \int_{\Omega} \left( \frac{1}{R^2} A_{22} \psi_3 \psi_3^T - A_{55} \psi_3 \psi_{3,11}^T - \frac{1}{R^2} A_{44} \psi_3 \psi_{3,22}^T + A_{11}^{\alpha} \Theta \psi_3 \psi_{3,11}^T \right. \\
&\quad \left. + \frac{2}{R} A_{12}^{\alpha} \Theta \psi_3 \psi_{3,12}^T + \frac{1}{R^2} A_{22}^{\alpha} \Theta \psi_3 \psi_{3,22}^T \right) d\Omega \\
K_{34} &= - \int_{\Omega} (A_{55} \psi_3 \psi_{4,1}^T) d\Omega, \quad K_{35} = - \int_{\Omega} \left( \frac{1}{R} A_{44} \psi_3 \psi_{5,2}^T \right) d\Omega \\
K_{43} &= \int_{\Omega} (A_{55} \psi_4 \psi_{3,1}^T) d\Omega \\
K_{44} &= \int_{\Omega} \left( D_{11} \psi_{4,1} \psi_{4,1}^T + A_{55} \psi_4 \psi_4^T - D_{66} \frac{1}{R^2} \psi_4 \psi_{4,22}^T \right) d\Omega \\
K_{45} &= \int_{\Omega} \left( D_{12} \frac{1}{R} \psi_{4,1} \psi_{5,2}^T - D_{66} \frac{1}{R} \psi_4 \psi_{5,12}^T \right) d\Omega \\
K_{53} &= \int_{\Omega} (A_{44} \psi_5 \psi_{3,2}^T) d\Omega, \quad K_{54} = \int_{\Omega} \left( D_{12} \frac{1}{R} \psi_{5,2} \psi_{4,1}^T - D_{66} \frac{1}{R} \psi_5 \psi_{4,12}^T \right) d\Omega \\
K_{55} &= \int_{\Omega} \left( D_{22} \frac{1}{R^2} \psi_{5,2} \psi_{5,2}^T + A_{44} \psi_5 \psi_5^T - D_{66} \psi_5 \psi_{5,11}^T \right) d\Omega \\
\int_{\Omega} d\Omega &= \int_0^{2\pi} \int_0^L dx d\theta
\end{aligned}$$